

---

# INVERSE DESIGN OF GRATING COUPLERS USING THE POLICY GRADIENT METHOD FROM REINFORCEMENT LEARNING

---

A PREPRINT

✉ **Sean Hooten\***  
 Hewlett Packard Labs  
 Hewlett Packard Enterprise  
 Milpitas, CA 95035, USA  
 shooten@eecs.berkeley.edu

**Raymond G. Beausoleil**  
 Hewlett Packard Labs  
 Hewlett Packard Enterprise  
 Milpitas, CA 95035, USA  
 ray.beausoleil@hpe.com

✉ **Thomas Van Vaerenbergh**  
 Hewlett Packard Labs  
 HPE Belgium  
 B-1831 Diegem, Belgium  
 thomas.van-vaerenbergh@hpe.com

November 2, 2021

## ABSTRACT

We present a proof-of-concept technique for the inverse design of electromagnetic devices motivated by the policy gradient method in reinforcement learning, named PHORCED (**PH**otonic **O**ptimization using **REINFORCE** Criteria for **E**nhanced **D**esign). This technique uses a probabilistic generative neural network interfaced with an electromagnetic solver to assist in the design of photonic devices, such as grating couplers. We show that PHORCED obtains better performing grating coupler designs than local gradient-based inverse design via the adjoint method, while potentially providing faster convergence over competing state-of-the-art generative methods. Furthermore, we implement transfer learning with PHORCED, demonstrating that a neural network trained to optimize  $8^\circ$  grating couplers can then be re-trained on grating couplers with alternate scattering angles while requiring  $>10\times$  fewer simulations than control cases.

**Keywords** artificial intelligence, reinforcement learning, machine learning, neural network, policy gradient, optimization, inverse design, adjoint method, physics, electromagnetics, photonics, grating coupler

## 1 Introduction

There has been a recent, massive surge in research syncretizing topics in photonics and artificial intelligence / machine learning (AI/ML), including photonic analog accelerators [1–8], physics emulators [9–15], and AI/ML-enhanced inverse electromagnetic design techniques [15–34]. While inverse electromagnetic design via local gradient-based optimization with the adjoint method has been successfully applied to a multitude of design problems throughout the entirety of the optics and photonics communities [35–59], inverse electromagnetic design leveraging AI/ML techniques promise superior computational performance, advanced data analysis and insight, or improved effort towards global optimization. For the lattermost topic in particular, Jiang and Fan recently introduced an unsupervised learning technique called GLOnet which uses a generative neural network interfaced with an electromagnetic solver to design photonic devices such as metasurfaces and distributed Bragg reflectors [23–25]. In this paper we propose a conceptually similar design technique, but with a contrasting theoretical implementation motivated by a concept in reinforcement learning called the policy gradient method – specifically a one-step implementation of the REINFORCE algorithm [60, 61]. We will refer to our technique as PHORCED = **PH**otonic **O**ptimization using **REINFORCE** Criteria for **E**nhanced **D**esign. PHORCED is compatible with any external physics solver including EMopt [62], a versatile electromagnetic optimization package that is employed in this work to perform 2D simulations of single-polarization grating couplers.

In Section 2, we will qualitatively compare and contrast three optimization techniques: local gradient-based optimization (e.g., gradient ascent), GLOnet, and PHORCED. We are specifically interested in a proof-of-concept demonstration of the PHORCED optimization technique applied to grating couplers, which we present in Section 3. We find that both our

---

\*Also affiliated with Department of Electrical Engineering and Computer Sciences, University of California, Berkeley, Berkeley, CA 94709, USA.

implementation of the GLOnet method and PHORCED find better grating coupler designs than local gradient-based optimization, but PHORCED requires fewer electromagnetic simulation evaluations than GLOnet. Finally, in Section 4 we introduce the concept of transfer learning to integrated photonic optimization for the first time to our knowledge, where in our application we demonstrate that a neural network trained to design  $8^\circ$  grating couplers with the PHORCED method can be re-trained to design grating couplers that scatter at alternate angles with greatly accelerated time-to-convergence. We speculate that a hierarchical optimization protocol leveraging this technique can be used to design computationally complex devices while minimizing computational overhead.

## 2 Extending the Adjoint Method with Neural Networks

Local gradient-based optimization using the adjoint method has been successfully applied to the design of a plethora of electromagnetic devices. Detailed tutorials of the adjoint method applied to electromagnetic optimization may be found in Refs. [35–38, 42, 45, 59]. Here, we qualitatively illustrate a conventional design loop utilizing the adjoint method in Fig. 1(a). This begins with the choice of an initial electromagnetic structure parameterized by vector  $\mathbf{p}$ , which might represent geometrical degrees-of-freedom like the width and height of the device. This is fed into an electromagnetic solver, denoted by a function  $g$ . The resulting electric and magnetic fields,  $\mathbf{x} = g(\mathbf{p})$ , can be used to evaluate a user-defined electromagnetic *merit function*  $f(\mathbf{x})$  – the metric that we are interested in optimizing (e.g., coupling efficiency). Gradient-based optimization seeks to improve the value of the merit function by updating the design parameters,  $\mathbf{p}$ , in a direction specified by the gradient of the electromagnetic merit function,  $\frac{\partial(f \circ g)}{\partial \mathbf{p}}$ . The value of the gradient may be obtained very efficiently using the adjoint method, requiring just two electromagnetic simulations regardless of the number of degrees-of-freedom (called the forward simulation and adjoint simulation, respectively). A single iteration of gradient-based optimization is depicted visually in the center of Fig. 1(a), where  $p$  is a single-dimension point sampled along a toy merit function  $(f \circ g)(p)$  representing the optimization landscape (which is unknown, a priori). The derivative (gradient) of the merit function is illustrated by the arrow pointing from  $p$  in the direction of steepest ascent (assuming this is a maximization problem). During an optimization, we slowly update  $p$  in this direction until a local optimum is reached.

The adjoint method chain-rule derivative of the electromagnetic merit function resembles the concept of *backpropagation* in deep learning, where a neural network’s weights can be updated efficiently using an application of the chain-rule with information from the forward pass. Naturally, we might extend the functionality of the adjoint method by placing a neural network in the design loop. The neural network takes the place of a deterministic update algorithm (such as gradient ascent), potentially learning information or patterns in the design problem that allows it to find a better optimum. We present two methods to implement inverse design with neural networks: GLOnet (introduced by Jiang and Fan [23, 24]) and PHORCED (this work). Both methods are qualitatively similar, but differ in the representation of the neural network.

The GLOnet optimization method is depicted qualitatively in Fig. 1(b). The neural network is represented as a deterministic function  $h_\theta$  that takes in noise  $\mathbf{z}$  from some known distribution  $D$  and outputs design parameters  $\mathbf{p}$ . Importantly, the neural network is parameterized by programmable weights  $\theta$  that we intend to optimize in order to generate progressively better electromagnetic devices. Similar to regular gradient ascent, we may evaluate the electromagnetic merit function of a device generated by the neural network  $(f \circ g)(\mathbf{p})$  using our physics solver, and find its gradient with respect to the design parameters using the adjoint method,  $\frac{\partial(f \circ g)}{\partial \mathbf{p}}$ . However, the GLOnet design problem is inherently stochastic because of the presence of noise, and therefore the “merit function” for optimization is the expected value of the electromagnetic merit function,  $\mathbb{E}_{\mathbf{z}}[(f \circ g \circ h_\theta)(\mathbf{z})]$  – sometimes called the *reward* in the reinforcement learning literature<sup>2</sup>. In practice this expression can be approximated by taking a simple average over the electromagnetic merit functions of several devices generated by the neural network per iteration. The gradient that is then backpropagated to the neural network is given by the expected value of the chain-rule gradient of the reward function. The first term,  $\frac{\partial(f \circ g)}{\partial \mathbf{p}}$ , can once again be computed very efficiently using the adjoint method, requiring just two electromagnetic simulations per device. Meanwhile the latter term,  $\frac{\partial h_\theta(\mathbf{z})}{\partial \theta}$ , can be calculated internal to the neural network using conventional backpropagation. Visually, one iteration of the GLOnet method is shown in the center of Fig. 1(b). In each iteration, the neural network in the GLOnet method suggests parameters,  $p_i$ , which are then individually simulated. Similar to gradient-based optimization from Fig. 1(a), we find the gradient of the merit function value with respect to each generated design parameter, represented by the arrows pointing towards the direction of steepest ascent at each point. The net gradient information from many simulated devices effectively tells the neural

<sup>2</sup>Note that we have written a generalized version of the reward function defined in the original works by Jiang and Fan [23, 24]. In that case, the reward function is chosen to weight good devices exponentially, i.e.  $f \rightarrow \exp(f/\sigma)$  where  $\sigma$  is a hyperparameter and  $f$  is the electromagnetic quantity of interest.

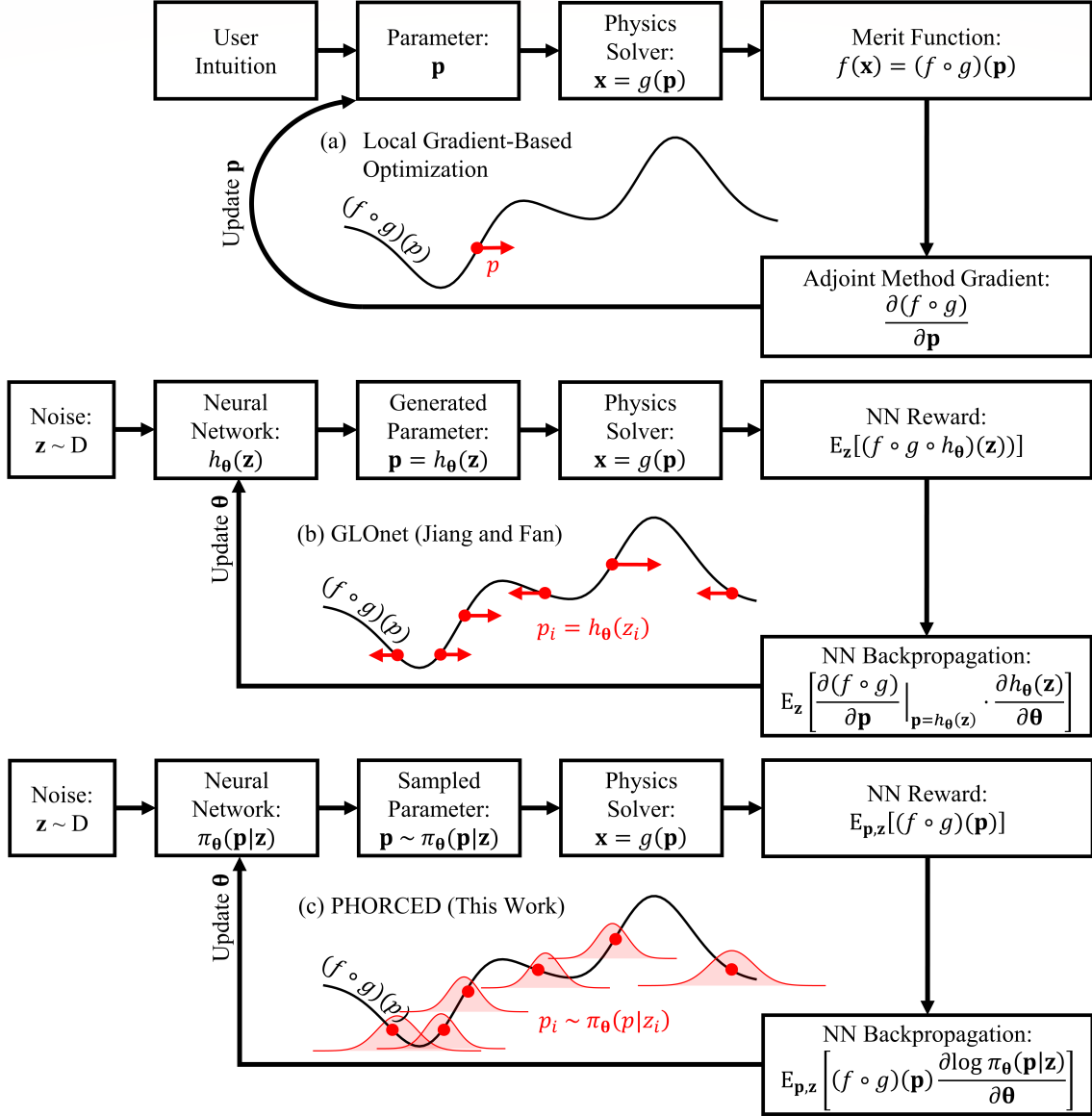


Figure 1: Neural networks provide a natural extension to conventional inverse design via the adjoint method. A typical gradient-based design loop is shown in (a) where the derivatives are calculated using the adjoint method. The GLOnet method (b), originally proposed by Jiang and Fan [23, 24], replaces a conventional gradient-based optimization algorithm with a deterministic neural network. In this work we propose PHORCED (c), which uses a probabilistic neural network to generate devices. (b) and (c) are qualitatively similar, but require different gradients in backpropagation because of the representation of the neural network (deterministic versus probabilistic). In particular, notice that PHORCED does not require an evaluation of the adjoint method gradient of the electromagnetic merit function,  $\frac{\partial(f \circ g)}{\partial \mathbf{p}}$ .

network where to explore in the next iteration. With a dense search, the global optimum along the domain of interest can potentially be found.

Our technique, called PHORCED, is provided in Fig. 1(c). Qualitatively speaking, it is very similar to GLOnet, but is motivated differently from a mathematical perspective. PHORCED is a special case of the REINFORCE algorithm [60, 61] from the field of reinforcement learning (RL), applied to electromagnetic inverse design. In particular, the neural network is treated as purely probabilistic, defining a continuous conditional probability density function over parameter variables  $\mathbf{p}$  conditioned on the input noise vector  $\mathbf{z}$  – denoted by  $\pi_{\theta}(\mathbf{p}|\mathbf{z})$ . In other words, instead of outputting  $\mathbf{p}$  deterministically given input noise, the neural network outputs probabilities of generating  $\mathbf{p}$ . We then randomly sample

a parameter vector  $\mathbf{p}$  for simulation and evaluation of the reward. Note that  $\pi_\theta(\mathbf{p}|\mathbf{z})$  is called the *policy* in RL, and in this work is chosen to be a multivariate Gaussian distribution with mean vector and standard deviation of random variable  $\mathbf{p}$  as outputs. The reward for PHORCED is qualitatively the same as GLOnet – namely, we intend to optimize the expected value of the electromagnetic merit function. However, because both  $\mathbf{p}$  and  $\mathbf{z}$  are random variables, we take the joint expected value:  $\mathbb{E}_{\mathbf{p},\mathbf{z}}[(f \circ g)(\mathbf{p})]$ . Furthermore, because of the probabilistic representation of the neural network, the gradient of the reward with respect to the neural net weights for backpropagation is much different than the corresponding GLOnet case. In particular, we find that the backpropagated chain-rule gradient requires **no evaluation** of the gradient of the electromagnetic merit function,  $\frac{\partial(f \circ g)}{\partial \mathbf{p}}$ . Consequently, the electromagnetic adjoint simulation is no longer required, implying that fewer simulations are required overall for PHORCED compared to GLOnet under equivalent choices of neural network architecture and hyperparameters<sup>3</sup>. PHORCED is visually illustrated in the center of Fig. 1(c). The neural network defines Gaussian probability density functions conditioned on input noise vectors  $z_i$ , shown in the light red bell curves representing  $\pi_\theta(p|z_i)$ , from which we sample points  $p_i$  to simulate. In our implementation we sample only one parameter vector per respective input noise vector conditioning the policy, though alternatively one could choose to sample multiple parameter vectors per policy<sup>4</sup>. Using information from the merit function values, the neural network learns to update the mean and standard deviation of the Gaussians. For adequate choice of distribution and dense enough search, the PHORCED method can potentially find the global optimum in the domain of interest.

Before proceeding it should be remarked that the algorithms implemented by GLOnet and PHORCED have precedent in the literature, with some distinctions that we will outline here. Optimization algorithms similar to GLOnet were suggested in Refs. [63, 64], where the main algorithmic difference appears in the definition of the reward function. In particular, the reward defined in Ref. [63] was the same generalized form that we have presented in Fig. 1(b), while Jiang and Fan emphasized the use of an exponentially-weighted reward to enhance global optimization efforts [24]. On the other hand, PHORCED was motivated as a special case of the REINFORCE algorithm [60, 61], but also resembles some versions of evolutionary strategy [63–66]. The main difference between PHORCED and evolutionary strategy (ignoring several heuristics) is the explicit use of a neural network to model the multivariate Gaussian policy distribution, albeit some recent works have used neural networks in their implementations of evolutionary strategy [64, 66] for different applications than those studied here. Furthermore, PHORCED does not require a Gaussian policy; any explicitly-defined probability distribution can be used as an alternative if desired. Beyond evolutionary strategy, a recent work in fluid dynamics [67] uses an algorithm akin to PHORCED called One-Step Proximal Policy Optimization (PPO-1) – a version of REINFORCE with a single policy,  $\pi_\theta$ , operating on parallel instances of the optimization problem. The main distinction between PPO-1 and PHORCED is that we have used an input noise vector  $\mathbf{z}$  to condition the output policy distribution,  $\pi_\theta(\mathbf{x}|\mathbf{z})$ , which effectively instantiates multiple distinct policies acting on parallel instances of the optimization problem. This potentially enables multi-modal exploration of the parameter space, bypassing a known issue of Bayesian optimization with Gaussian probability distributions [64]. Nevertheless, further quantitative tests will be necessary to evaluate the performance differences between PHORCED and PPO-1. Regardless of the intricacies mentioned above, we emphasize that both GLOnet and PHORCED are unique in their application to electromagnetic optimization, to the authors’ knowledge. In the next section we will compare all three algorithms from Fig. 1 applied to grating coupler optimization.

### 3 Proof-of-Concept Grating Coupler Optimization

A grating coupler is a passive photonic device that is capable of scattering light from an on-chip waveguide to an external optical fiber efficiently. Recent works have leveraged inverse design techniques in the engineering of grating couplers, resulting in state-of-the-art characteristics [20, 41, 43, 51, 55]. In this section we will show how generative neural networks can aid in the design of ultra-efficient grating couplers.

The grating coupler geometry used for our proof-of-concept is depicted in Fig. 2(a). We assume a silicon-on-insulator (SOI) wafer platform with a 304nm-thick silicon waveguide separated from the silicon substrate by a 2 $\mu\text{m}$  buried oxide (BOX) layer. The grating coupler consists of periodically spaced corrugations to the input silicon waveguide with etch depth 159nm. For our optimizations, we will consider 60 total designable parameters that define the grating coupler: the width of and spacing between 30 waveguide corrugations. For a well-designed grating coupler, input light to the waveguide scatters at some angle relative to vertical toward an external optical fiber. In our case, the merit function for optimization is the coupling efficiency of scattered light with wavelength  $\lambda = 1550\text{nm}$  propagating 8° relative to normal, mode-matched to an output Gaussian beam with waist 10.4 $\mu\text{m}$  – characteristic of a typical optical fiber mode.

<sup>3</sup>However, because the representation of the neural network is different in either case, it would rarely make sense to use equivalent choices of neural network architecture and hyperparameters. Therefore, we make this claim tepidly, emphasizing only that we do not require adjoint simulations in the evaluation of the reward.

<sup>4</sup>This constitutes an additional hyperparameter that was not tested extensively in this work.

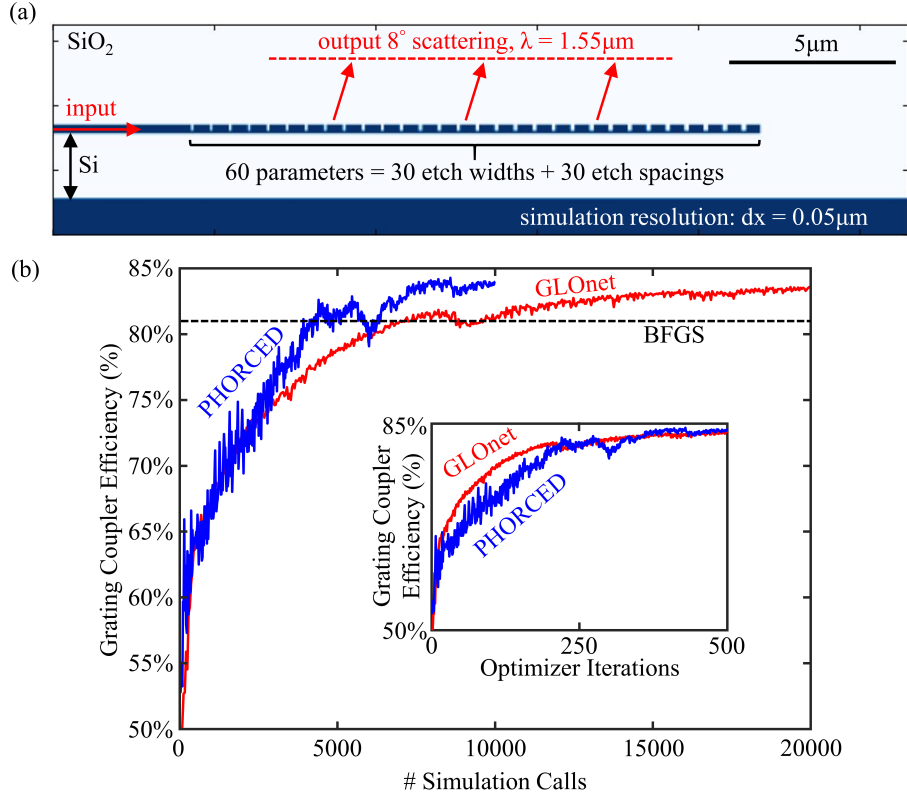


Figure 2: PHORCED and GLOnet outperform conventional gradient-based optimization, with different simulation evaluation requirements. The grating coupler simulation geometry for optimization is shown in (a), consisting of a SOI wafer platform with 304nm waveguide and 2 $\mu$ m BOX height. We optimized 60 device parameters in total, namely the width and spacing between 30 etch corrugations. The results of the BFGS, GLOnet, and PHORCED algorithms are presented in (b) as a function of the number of simulation calls. The inset depicts the same data, but plotted as a function of the optimizer iterations – 500 total for both GLOnet and PHORCED.

The explicit definition of this electromagnetic merit function may be found in Refs. [43, 51, 68]. Note that we did not include fabrication constraints nor other specifications of interest in grating couplers in our parameterization choice, e.g. the BOX thickness and the Si etch depth, which will be desirable in future optimizations of experimentally-viable devices. Furthermore, the simulation domain is discretized with a  $dx = 50$ nm grid step which may result in some inaccuracy for very fine grating coupler features. This simulation discretization was chosen for feasibility of the optimization since individual simulations require a few seconds to compute even on a high-performance server with over 20 concurrent MPI processes, and as we will show GLOnet and PHORCED can require as many as 20,000 simulation evaluations for convergence. Nevertheless, we utilized permittivity smoothing [42] to minimize the severity of this effect and obtain physically meaningful results.

We apply the BFGS, GLOnet, and PHORCED algorithms to grating coupler design in Fig. 2(b). BFGS (Broyden–Fletcher–Goldfarb–Shanno) is a conventional gradient-based optimization algorithm implemented similarly to that depicted in Fig. 1(a). The initial condition for BFGS optimization was a grating coupler with uniform pitch and a linear ramp in duty cycle (depicted in Fig. 2(a)), with corresponding grating coupler efficiency of approximately 64%. After optimization with BFGS, the final simulated grating coupler efficiency was approximately 81%. Note that the number of simulation calls for BFGS is not shown because it is vastly smaller than that required for GLOnet and PHORCED ( $\sim 50$ ). GLOnet is described qualitatively in Fig. 1(b) where we use a deterministic neural network and an exponentially-weighted electromagnetic merit function originally recommended by Jiang and Fan [23, 24] with a chosen hyperparameter  $\sigma = 0.6$ . PHORCED was described qualitatively in Fig. 1(c) where we use a probabilistic neural network modeling a multivariate, isotropic Gaussian output distribution. The electromagnetic merit function used in the reward is just the unweighted grating coupler efficiency, except we used a “baseline” subtraction of the average merit function value in the backpropagated gradient (which is a common tactic in reinforcement learning for reducing variance). We find that both PHORCED and GLOnet outperform regular BFGS in terms of grating coupler

efficiency with 84.3% and 83.6% respectively. However, PHORCED achieves the highest efficiency with fewer overall simulation calls. Note that Fig. 2(b) gives the results of our best optimization of these devices using each algorithm with varied hyperparameters and neural network architectures. In particular, we used a convolutional neural network with ReLU activations for GLOnet optimization and a simple fully-connected neural network with ReLU activations for PHORCED, where hyperparameters were individually tuned for each algorithm<sup>5</sup>. As shown in the inset of Fig. 2(b), both optimizations were performed with 500 overall iterations (using the Adam optimizer with tuned constant learning rate in each case), each with a batch size of 20 devices simulated per iteration. However, because PHORCED does not require an adjoint simulation evaluation,  $2\times$  fewer simulation calls were performed overall. While not included in this paper for brevity and lack of generality, we conducted optimizations using both algorithms with the exact same neural network architectures, ultimately finding that PHORCED was more robust and consistently provided better results in the grating coupler example studied here.

## 4 Transfer Learning with the PHORCED Method

Transfer learning is a concept in machine learning encompassing any method that reuses a model (e.g. a neural network) trained on one task for a different but related task. Qualitatively speaking and verified by real-world applications, we might expect the re-training of a neural network to occur faster than training a new model from scratch. Transfer learning has been extensively applied in classical machine learning tasks such as classification and regression, but has only recently been mentioned in the optics/photonics research domains [17, 26, 27, 32]. In this work we apply transfer learning to the inverse design of integrated photonics for the first time (to the authors’ knowledge), revealing that a neural network trained using PHORCED for the design of  $8^\circ$  grating couplers can be re-trained to design grating couplers with varied scattering angle and increased rate of convergence.

Transfer learning applied to grating coupler optimization is qualitatively illustrated in Fig. 3(a)-(b). Fig. 3(a) shows a shorthand version of the optimization that was performed in Fig. 2(b), where a neural network was specifically trained to design an  $8^\circ$  grating coupler. In the case of transfer learning in Fig. 3(b), we re-use the trained neural network from Fig. 3(a) but now exchange the  $8^\circ$  angle in the grating coupler efficiency merit function with an alternate scattering angle. In particular, we re-train the neural network on 6 alternative grating coupler angles:  $\{2^\circ, 4^\circ, 6^\circ, 10^\circ, 12^\circ, 14^\circ\}$ . Note that we maintained the exact same neural network architecture and optimization hyperparameters during these exchanges; the only change in a given optimization was the grating coupler angle. As depicted in Fig. 3(c), we show the optimization progressions of these transfer learning sessions (blue/red curves) in comparison to the original PHORCED optimization of the  $8^\circ$  grating coupler from Fig. 2(b) (reproduced in the black curve in the middle panel). Also shown are control optimizations for each grating coupler angle using the PHORCED method without transfer learning (in gray). We find that transfer learning to grating couplers with nearby scattering angles (e.g.  $6^\circ$  and  $10^\circ$ ) exhibit extremely accelerated rate of convergence relative to the original optimization and control cases. However, transfer learning is less effective for more distant angles (e.g.  $2^\circ$  and  $14^\circ$ ). This observation is shown more clearly in Fig. 3(d) where we plot the number of simulations required to reach 80% efficiency in optimization versus the scattering angle for re-training<sup>6</sup>. While the original optimization and control optimizations (black star and gray diamonds) required several thousand simulation calls before reaching this threshold, the  $6^\circ$  and  $10^\circ$  transfer learning optimizations required only about 100 simulations a piece – a  $>10\times$  reduction in simulation calls, making transfer learning comparable with local gradient-based optimization in terms of computation requirements. On the other hand, the distant grating coupler angle transfer learning optimizations ( $2^\circ$  and  $14^\circ$ ) required similar simulation call requirements to reach the same threshold as the original optimization, but still outperformed the control cases. We conclude that the transfer learning approach is most effective for devices with very similar physics to the device originally optimized by the neural network<sup>7</sup>.

The results of Fig. 3 lead to a natural follow-up query: can we apply transfer learning multiple times progressively in order to maintain the convergence rate advantage for optimizations at more distant grating coupler angles? We explore this question of *sequential* transfer learning in Fig. 4. In Fig. 4(a)-(b) we qualitatively compare sequential transfer learning to the original PHORCED optimization from Fig. 2(b). As indicated, we replace the original  $8^\circ$  grating coupler scattering angle in the electromagnetic merit function with an alternative scattering angle in the same manner discussed in Fig. 3(b). Then, after that optimization has completed, we continue to iterate and exchange the grating coupler angle again. By sequentially applying transfer learning, we hope to slowly introduce new physics to

<sup>5</sup>Note that we were unable to perform exhaustive hyperparameter testing in this work due to the prohibitively slow speed of electromagnetic simulations of this size. Indeed, a single optimization with the GLOnet method required as long as 24 hours on a high-performance server.

<sup>6</sup>80% grating coupler efficiency was chosen because it equates to roughly 1dB insertion loss – an optimistic target for state-of-the-art silicon photonic devices.

<sup>7</sup>It may be possible to train more generalizable models by using variance reduction methods. We relegate this possibility to future work.

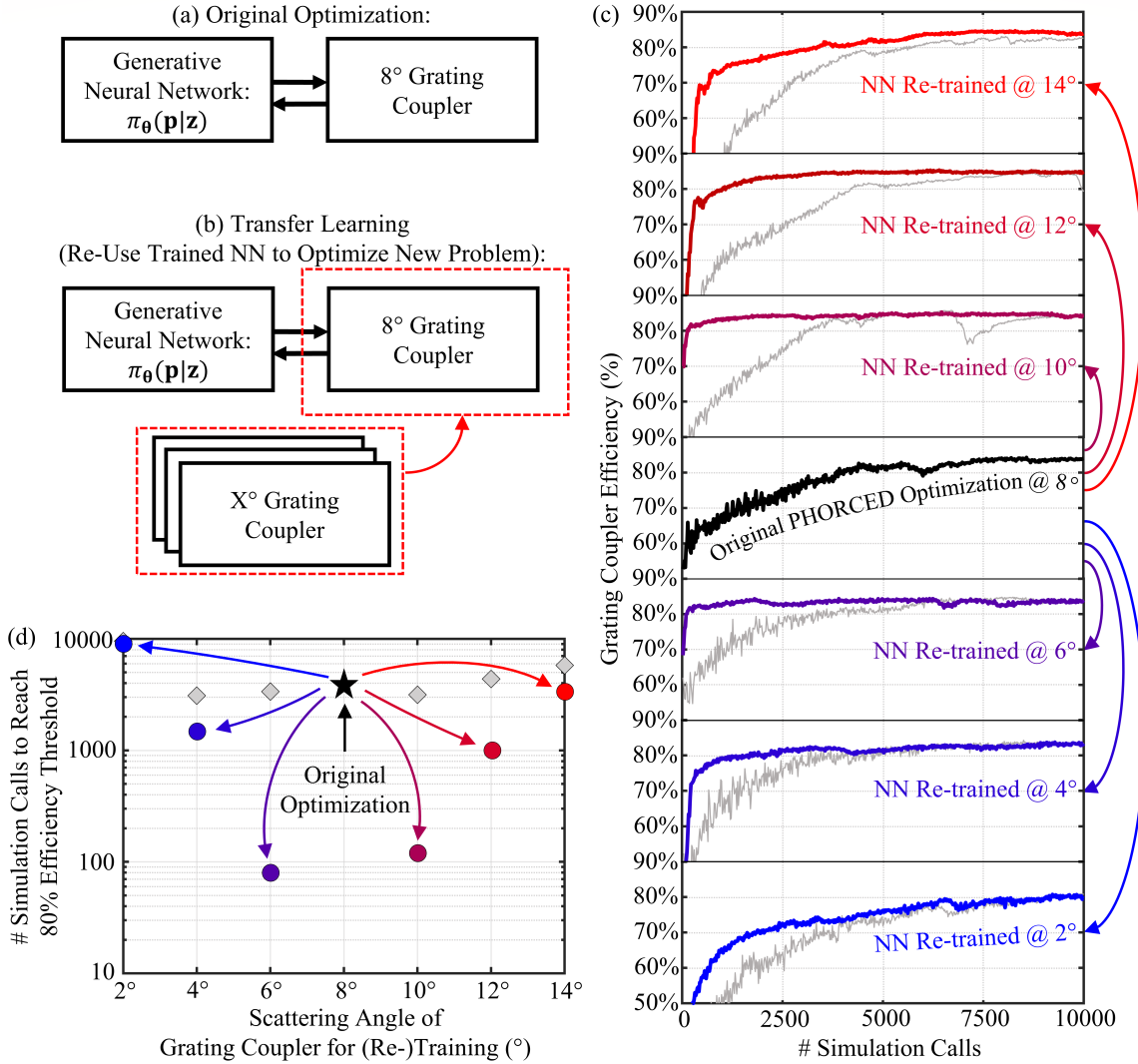


Figure 3: Transfer learning applied to grating coupler design yields accelerated convergence rate in optimization. The original PHORCED optimization from Fig. 2(b) is qualitatively depicted as a block diagram in (a) for comparison with the transfer learning approach in (b). Here, we exchange the 8° grating coupler merit function with an alternative grating coupler angle for re-training. Optimization progressions as a function of the number of simulation calls for each of the re-training sessions are shown in the blue/red curves of (c). Control optimizations where transfer learning was not applied are plotted in gray for comparison. In (d) we plot the number of simulation calls for each optimization from (c) to reach 80% grating coupler scattering efficiency, with blue/red colored arrows and dots indicating applications of transfer learning and gray diamonds indicating the control cases.

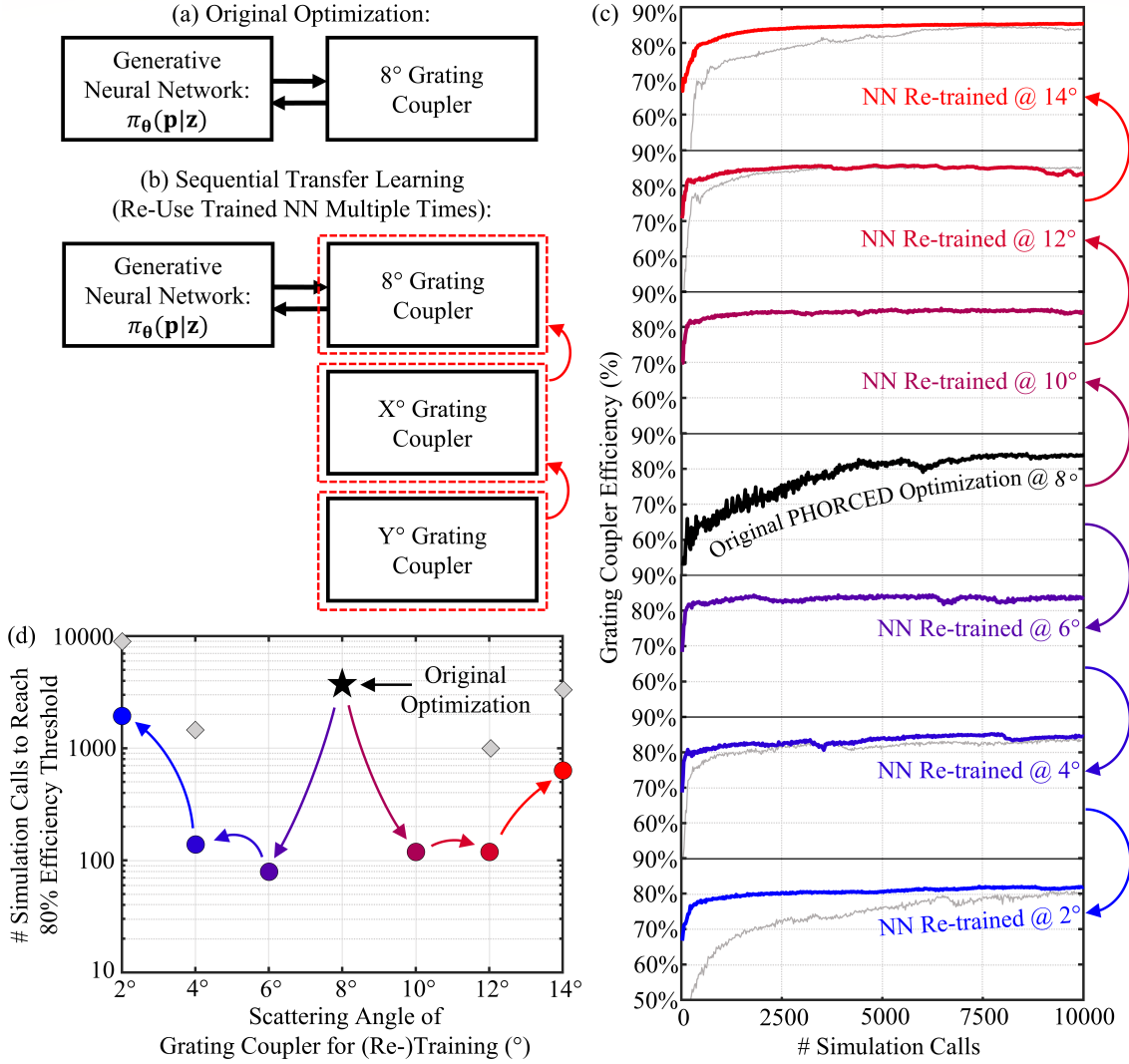


Figure 4: Transfer learning applied sequentially improves convergence for grating coupler scattering angles that are distant relative to the original optimization’s scattering angle. The original PHORCED optimization from Fig. 2(b) is qualitatively depicted in (a) for comparison with the “sequential” transfer learning approach in (b). Here, we sequentially re-train the neural network (originally trained to generate 8° grating couplers) with progressively different scattering angles, with the intention of slowly changing the physics seen by the neural network. Grating coupler efficiency as a function of the number of simulation calls for each of the re-training sessions are shown in the blue/red curves of (c), where the arrows on the right-hand side show the sequence of each application of transfer learning. The results of the one-shot (non-sequential) transfer learning approach from Fig. 3(c) are shown in gray for comparison. In (d) we plot the number of simulation calls needed for the grating coupler optimizations from (c) to reach an 80% efficiency using the sequential transfer learning approach, similar to the corresponding plot in Fig. 3(d). The blue/red arrows and dots indicate applications of sequential transfer learning, and the gray diamonds correspond to non-sequential transfer learning cases.



the neural network such that we can maintain faster convergence at more physically distant problems from the initial optimization. We conduct two sequential transfer learning sessions where we evolve the grating coupler scattering angle in the following ways:  $\{8^\circ \rightarrow 10^\circ \rightarrow 12^\circ \rightarrow 14^\circ\}$  and  $\{8^\circ \rightarrow 6^\circ \rightarrow 4^\circ \rightarrow 2^\circ\}$ . The results of these progressions are shown in Fig. 4(c) where we plot the grating coupler efficiency as a function of the number of simulation calls in each (re-)training session. The  $6^\circ$ ,  $8^\circ$ , and  $10^\circ$  cases are the same as those shown previously in Fig. 3(c); the new results may be seen in the  $2^\circ$ ,  $4^\circ$ ,  $12^\circ$ , and  $14^\circ$  cases, where blue/red lines indicate the new optimization data and gray lines indicate the non-sequential transfer learning cases from Fig. 3(c) for comparison. We observe that sequential transfer learning improves the optimization convergence rate for the distant grating coupler scattering angles, in accordance with our initial prediction. This observation is made more explicit in Fig. 4(d) where we plot the simulation call requirement to reach an 80% grating coupler efficiency threshold for each of the transfer learning optimizations. Blue/red arrows and points indicate sequential transfer learning progressions, while gray diamonds indicate the one-shot transfer learning cases reproduced from Fig. 3(d). Evidently, sequential transfer learning improves simulation call requirements by nearly an order of magnitude in these cases. Note that the plotted simulation call requirements do not include the simulation calls from the previous iteration in the sequential transfer learning progression (each application of transfer learning used 10,000 simulation calls, where the final neural network weightset after those 10,000 simulation calls was used as the initial weightset for the next iteration of transfer learning). Furthermore, note that each optimization in these sequential transfer learning cases used the same neural network architecture and hyperparameters as the original PHORCED optimization ( $8^\circ$  case), except for the  $\{12^\circ \rightarrow 14^\circ\}$  and  $\{4^\circ \rightarrow 2^\circ\}$  cases which required a slightly smaller learning rate in optimization for better performance. The smaller learning rate negligibly affected the 80% efficiency simulation call requirement shown in Fig. 4(d).

## 5 Conclusion

In this work we introduced PHORCED, a photonic optimization package leveraging the policy gradient method from reinforcement learning. This method interfaces a probabilistic neural network with an electromagnetic solver for enhanced inverse design capabilities. PHORCED does not require an evaluation of adjoint method gradient of the electromagnetic merit function with respect to the design parameters, therefore eliminating the need to perform adjoint simulations over the course of an optimization. We anticipate that this fact can be particularly advantageous for multi-frequency electromagnetic merit functions, where multiple adjoint simulations would normally be required in a simple frequency-domain implementation of the adjoint method (e.g., see Ref. [51]).

We applied both PHORCED and the GLOnet method to the proof-of-concept optimization of grating couplers, finding that both algorithms could outperform conventional gradient-based BFGS optimization, resulting in state-of-the-art simulated insertion loss for single-etch c-Si grating couplers. In future work we intend to implement fabrication constraints, alternative choices of geometrical parameterization, and other criteria to guarantee feasibility and robustness of experimental devices.

As an additional contribution we introduced the concept of transfer learning to integrated photonic optimization, revealing that a trained neural network using PHORCED could be re-trained on alternative problems with accelerated convergence. In particular, we showed that transfer learning could be applied to the design of grating couplers with varied scattering angle. Transfer learning was extremely effective for grating coupler scattering angles within  $\approx \pm 4^\circ$  to the original optimization angle, improving the convergence rate by  $>10\times$  in some cases. However, this range could be effectively extended to  $\approx \pm 6^\circ$  or more using a sequential transfer learning approach, where transfer learning was applied multiple times progressively to slowly change the angle seen by the neural network. Because neural network based design methods such as PHORCED are generally data-hungry, we believe that transfer learning could greatly reduce the electromagnetic simulation and compute time that would otherwise be required by these techniques in the design of complex electromagnetic structures. For example, transfer learning could be used in multiple hierarchical stages to evolve an optimization from a two-dimensional structure to a three-dimensional structure, or from a surrogate model (e.g., the grating coupler model in Ref. [10]) to real physics.

Looking forward, we would like to emphasize that PHORCED takes advantage of fundamental concepts in reinforcement learning, but there is a plethora of burgeoning contemporary research in this field, such as advanced policy gradient, off-policy, and model-based approaches. We anticipate that further cross-pollination of the inverse electromagnetic design and reinforcement learning communities could open the floodgates for new research in electromagnetic optimization.

## References

- [1] Y. Shen, N. C. Harris, S. Skirlo, M. Prabhu, T. Baehr-Jones, M. Hochberg, X. Sun, S. Zhao, H. Larochelle, D. Englund, and M. Soljacic, “Deep Learning with Coherent Nanophotonic Circuits,” *Nature Photonics*, vol. 11, no. June, 2016. DOI: 10.1038/nphoton.2017.93.
- [2] T. Inagaki, Y. Haribara, K. Igarashi, T. Sonobe, S. Tamate, T. Honjo, A. Marandi, P. L. McMahon, T. Umeki, K. Enbutsu, O. Tadanaga, H. Takenouchi, K. Aihara, K.-i. Kawarabayashi, K. Inoue, S. Utsunomiya, and H. Takesue, “A coherent Ising machine for 2000-node optimization problems,” *Science*, vol. 4243, no. October, 2016. DOI: 10.1126/science.aah4243.
- [3] N. C. Harris, G. R. Steinbrecher, M. Prabhu, Y. Lahini, J. Mower, D. Bunandar, C. Chen, F. N. Wong, T. Baehr-Jones, M. Hochberg, S. Lloyd, and D. Englund, “Quantum transport simulations in a programmable nanophotonic processor,” *Nature Photonics*, vol. 11, no. 7, pp. 447–452, 2017. DOI: 10.1038/nphoton.2017.95.
- [4] Y. Yamamoto, K. Aihara, T. Leleu, K.-i. Kawarabayashi, S. Kako, M. Fejer, K. Inoue, and H. Takesue, “Coherent Ising machines—optical neural networks operating at the quantum limit,” *npj Quantum Information*, vol. 3, no. 1, pp. 1–15, Dec. 2017. DOI: 10.1038/s41534-017-0048-9.
- [5] E. Khoram, A. Chen, D. Liu, L. Ying, Q. Wang, M. Yuan, and Z. Yu, “Nanophotonic media for artificial neural inference,” *Photonics Research*, vol. 7, no. 8, 2018. DOI: 10.1364/prj.7.000823.
- [6] T. W. Hughes, I. A. D. Williamson, M. Minkov, and S. Fan, “Wave physics as an analog recurrent neural network,” *Science Advances*, vol. 5, no. 12, 2019. DOI: 10.1126/sciadv.aay6946.
- [7] B. J. Shastri, A. N. Tait, T. Ferreira de Lima, W. H. P. Pernice, H. Bhaskaran, C. D. Wright, and P. R. Prucnal, “Photonics for artificial intelligence and neuromorphic computing,” *Nature Photonics*, vol. 15, no. 2, pp. 102–114, Feb. 2021. DOI: 10.1038/s41566-020-00754-y.
- [8] X. Xu, M. Tan, B. Corcoran, J. Wu, A. Boes, T. G. Nguyen, S. T. Chu, B. E. Little, D. G. Hicks, R. Morandotti, A. Mitchell, and D. J. Moss, “11 TOPS photonic convolutional accelerator for optical neural networks,” *Nature*, vol. 589, no. 7840, pp. 44–51, Jan. 2021. DOI: 10.1038/s41586-020-03063-0.
- [9] M. Raissi, P. Perdikaris, and G. E. Karniadakis, “Physics-informed neural networks: A deep learning framework for solving forward and inverse problems involving nonlinear partial differential equations,” *Journal of Computational Physics*, vol. 378, pp. 686–707, 2019. DOI: <https://doi.org/10.1016/j.jcp.2018.10.045>.
- [10] D. Gostimirovic and W. N. Ye, “An Open-Source Artificial Neural Network Model for Polarization-Insensitive Silicon-on-Insulator Subwavelength Grating Couplers,” *IEEE Journal of Selected Topics in Quantum Electronics*, vol. 25, no. 3, pp. 1–5, May 2019. DOI: 10.1109/JSTQE.2018.2885486.
- [11] Y. Guo, X. Cao, B. Liu, and M. Gao, “Solving Partial Differential Equations Using Deep Learning and Physical Constraints,” *Applied Sciences*, vol. 10, no. 17, p. 5917, Jan. 2020. DOI: 10.3390/app10175917.
- [12] Y. Chen, L. Lu, G. E. Karniadakis, and L. D. Negro, “Physics-informed neural networks for inverse problems in nano-optics and metamaterials,” *Optics Express*, vol. 28, no. 8, pp. 11 618–11 633, Apr. 2020. DOI: 10.1364/OE.384875.
- [13] R. Pestourie, Y. Mroueh, T. V. Nguyen, P. Das, and S. G. Johnson, “Active learning of deep surrogates for PDEs: Application to metasurface design,” *npj Computational Materials*, vol. 6, no. 1, pp. 1–7, Oct. 2020. DOI: 10.1038/s41524-020-00431-2.
- [14] A. Ghosh, D. J. Roth, L. H. Nicholls, W. P. Wardley, A. V. Zayats, and V. A. Podolskiy, “Machine Learning-Based Diffractive Image Analysis with Subwavelength Resolution,” *ACS Photonics*, vol. 8, no. 5, pp. 1448–1456, May 2021. DOI: 10.1021/acsp Photonics.1c00205.
- [15] L. Lu, R. Pestourie, W. Yao, Z. Wang, F. Verdugo, and S. G. Johnson, “Physics-informed neural networks with hard constraints for inverse design,” *arXiv:2102.04626 [physics]*, Feb. 2021.
- [16] R. Trivedi, L. Su, J. Lu, M. F. Schubert, and J. Vuckovic, “Data-driven acceleration of photonic simulations,” *Scientific Reports*, vol. 9, no. 1, pp. 1–7, 2019. DOI: 10.1038/s41598-019-56212-5.
- [17] Y. Qu, L. Jing, Y. Shen, M. Qiu, and M. Soljačić, “Migrating Knowledge between Physical Scenarios Based on Artificial Neural Networks,” *ACS Photonics*, vol. 6, no. 5, pp. 1168–1174, May 2019. DOI: 10.1021/acsp Photonics.8b01526.
- [18] D. Melati, Y. Grinberg, M. Kamandar Dezfouli, S. Janz, P. Cheben, J. H. Schmid, A. Sánchez-Postigo, and D. X. Xu, “Mapping the global design space of nanophotonic components using machine learning pattern recognition,” *Nature Communications*, vol. 10, no. 1, pp. 1–9, 2019. DOI: 10.1038/s41467-019-12698-1.
- [19] A. Demeter-Finzi and S. Ruschin, “S-matrix absolute optimization method for a perfect vertical waveguide grating coupler,” *Optics Express*, vol. 27, no. 12, pp. 16 713–16 718, Jun. 2019. DOI: 10.1364/OE.27.016713.

- [20] M. K. Dezfouli, Y. Grinberg, D. Melati, J. H. Schmid, P. Cheben, S. Janz, and D.-X. Xu, “Design of fully apodized and perfectly vertical surface grating couplers using machine learning optimization,” in *Integrated Optics: Devices, Materials, and Technologies XXV*, vol. 11689, International Society for Optics and Photonics, Mar. 2021, 116890J. DOI: 10.1117/12.2576945.
- [21] M. M. R. Elsayy, S. Lanteri, R. Duvigneau, G. Brière, M. S. Mohamed, and P. Genevet, “Global optimization of metasurface designs using statistical learning methods,” *Scientific Reports*, vol. 9, no. 1, p. 17918, Nov. 2019. DOI: 10.1038/s41598-019-53878-9.
- [22] A. M. Hammond and R. M. Camacho, “Designing integrated photonic devices using artificial neural networks,” *Optics Express*, vol. 27, no. 21, pp. 29620–29638, Oct. 2019. DOI: 10.1364/OE.27.029620.
- [23] J. Jiang and J. A. Fan, “Global Optimization of Dielectric Metasurfaces Using a Physics-Driven Neural Network,” *Nano Letters*, vol. 19, no. 8, pp. 5366–5372, Aug. 2019. DOI: 10.1021/acs.nanolett.9b01857.
- [24] J. Jiang and J. A. Fan, “Simulator-based training of generative neural networks for the inverse design of metasurfaces,” *Nanophotonics*, vol. 9, no. 5, pp. 1059–1069, 2020. DOI: doi:10.1515/nanoph-2019-0330.
- [25] J. Jiang and J. A. Fan, “Multiobjective and categorical global optimization of photonic structures based on ResNet generative neural networks,” *Nanophotonics*, vol. 10, no. 1, pp. 361–369, Sep. 2020. DOI: doi:10.1515/nanoph-2020-0407.
- [26] J. Jiang, M. Chen, and J. A. Fan, “Deep neural networks for the evaluation and design of photonic devices,” *Nature Reviews Materials*, pp. 1–22, Dec. 2020. DOI: 10.1038/s41578-020-00260-1.
- [27] R. S. Hegde, “Deep learning: A new tool for photonic nanostructure design,” *Nanoscale Advances*, vol. 2, no. 3, pp. 1007–1023, 2020. DOI: 10.1039/c9na00656g.
- [28] M. Minkov, I. A. Williamson, L. C. Andreani, D. Gerace, B. Lou, A. Y. Song, T. W. Hughes, and S. Fan, “Inverse Design of Photonic Crystals through Automatic Differentiation,” *ACS Photonics*, vol. 7, no. 7, pp. 1729–1741, 2020. DOI: 10.1021/acsphotonics.0c00327.
- [29] S. So, T. Badloe, J. Noh, J. Rho, and J. Bravo-Abad, “Deep learning enabled inverse design in nanophotonics,” *Nanophotonics*, vol. 2234, pp. 1–17, 2020. DOI: 10.1515/nanoph-2019-0474.
- [30] Z. Ma and Y. Li, “Parameter extraction and inverse design of semiconductor lasers based on the deep learning and particle swarm optimization method,” *Optics Express*, vol. 28, no. 15, p. 21971, 2020. DOI: 10.1364/oe.389474.
- [31] K. Kojima, M. H. Tahersima, T. Koike-Akino, D. K. Jha, Y. Tang, Y. Wang, and K. Parsons, “Deep Neural Networks for Inverse Design of Nanophotonic Devices,” *Journal of Lightwave Technology*, vol. 39, no. 4, pp. 1010–1019, Feb. 2021. DOI: 10.1109/JLT.2021.3050083.
- [32] W. Ma, Z. Liu, Z. A. Kudyshev, A. Boltasseva, W. Cai, and Y. Liu, “Deep learning for the design of photonic structures,” *Nature Photonics*, vol. 15, no. 2, pp. 77–90, 2021. DOI: 10.1038/s41566-020-0685-y.
- [33] D. Melati, M. Kamandar Dezfouli, Y. Grinberg, J. H. Schmid, R. Cheriton, S. Janz, P. Cheben, and D. X. Xu, “Design of Compact and Efficient Silicon Photonic Micro Antennas with Perfectly Vertical Emission,” *IEEE Journal of Selected Topics in Quantum Electronics*, vol. 27, no. 1, 2021. DOI: 10.1109/JSTQE.2020.3013532.
- [34] R. Hegde, “Sample-efficient deep learning for accelerating photonic inverse design,” *OSA Continuum*, vol. 4, no. 3, pp. 1019–1033, Mar. 2021. DOI: 10.1364/OSAC.420977.
- [35] J. S. Jensen and O. Sigmund, “Topology optimization for nano-photonics,” *Laser and Photonics Reviews*, vol. 5, no. 2, pp. 308–321, 2011. DOI: 10.1002/lpor.201000014.
- [36] J. Lu and J. Vučković, “Objective-first design of high-efficiency, small-footprint couplers between arbitrary nanophotonic waveguide modes,” *Optics Express*, vol. 20, no. 7, pp. 7221–7236, Mar. 2012. DOI: 10.1364/OE.20.007221.
- [37] C. M. Lalau-Keraly, S. Bhargava, O. D. Miller, and E. Yablonovitch, “Adjoint shape optimization applied to electromagnetic design,” *Optics Express*, vol. 21, no. 18, pp. 21693–21701, Sep. 2013. DOI: 10.1364/OE.21.021693.
- [38] Y. Elesin, B. S. Lazarov, J. S. Jensen, and O. Sigmund, “Time domain topology optimization of 3D nanophotonic devices,” *Photonics and Nanostructures - Fundamentals and Applications*, vol. 12, no. 1, pp. 23–33, Feb. 2014. DOI: 10.1016/j.photonics.2013.07.008.
- [39] A. Y. Piggott, J. Lu, K. G. Lagoudakis, J. Petykiewicz, T. M. Babinec, and J. Vučković, “Inverse design and demonstration of a compact and broadband on-chip wavelength demultiplexer,” *Nature Photonics*, vol. 9, no. 6, pp. 374–377, Jun. 2015. DOI: 10.1038/nphoton.2015.69.
- [40] L. F. Frellsen, Y. Ding, O. Sigmund, and L. H. Frandsen, “Topology optimized mode multiplexing in silicon-on-insulator photonic wire waveguides,” *Optics Express*, vol. 24, no. 15, pp. 16866–16873, Jul. 2016. DOI: 10.1364/OE.24.016866.

- [41] L. Su, R. Trivedi, N. V. Sapra, A. Y. Piggott, D. Vercruyssen, and J. Vučković, “Fully-automated optimization of grating couplers,” *Optics Express*, vol. 26, no. 4, pp. 2614–2617, 2017. DOI: 10.1364/OE.26.004023.
- [42] A. Michaels and E. Yablonovitch, “Leveraging continuous material averaging for inverse electromagnetic design,” *Optics Express*, vol. 26, no. 24, pp. 31 717–31 737, Nov. 2018. DOI: 10.1364/OE.26.031717.
- [43] A. Michaels and E. Yablonovitch, “Inverse design of near unity efficiency perfectly vertical grating couplers,” *Optics Express*, vol. 26, no. 4, pp. 4766–4779, Feb. 2018. DOI: 10.1364/OE.26.004766.
- [44] S. Molesky, Z. Lin, A. Y. Piggott, W. Jin, J. Vucković, and A. W. Rodriguez, “Inverse design in nanophotonics,” *Nature Photonics*, vol. 12, no. 11, pp. 659–670, Nov. 2018. DOI: 10.1038/s41566-018-0246-9.
- [45] T. W. Hughes, M. Minkov, I. A. D. Williamson, and S. Fan, “Adjoint Method and Inverse Design for Non-linear Nanophotonic Devices,” *ACS Photonics*, vol. 5, no. 12, pp. 4781–4787, Dec. 2018. DOI: 10.1021/acsp Photonics.8b01522.
- [46] Y. Liu, W. Sun, H. Xie, N. Zhang, K. Xu, Y. Yao, S. Xiao, and Q. Song, “Very sharp adiabatic bends based on an inverse design,” *Opt. Lett.*, vol. 43, no. 11, pp. 2482–2485, 2018. DOI: 10.1364/OL.43.002482.
- [47] N. M. Andrade, S. Hooten, S. A. Fortuna, K. Han, E. Yablonovitch, and M. C. Wu, “Inverse design optimization for efficient coupling of an electrically injected optical antenna-LED to a single-mode waveguide,” *Optics Express*, vol. 27, no. 14, pp. 19 802–19 814, Jul. 2019. DOI: 10.1364/OE.27.019802.
- [48] D. Vercruyssen, N. V. Sapra, L. Su, R. Trivedi, and J. Vučković, “Analytical level set fabrication constraints for inverse design,” *Scientific Reports*, vol. 9, no. 1, pp. 1–7, 2019. DOI: 10.1038/s41598-019-45026-0.
- [49] Y. Augenstein and C. Rockstuhl, “Inverse Design of Nanophotonic Devices with Structural Integrity,” *ACS Photonics*, vol. 7, no. 8, pp. 2190–2196, 2020. DOI: 10.1021/acsp Photonics.0c00699.
- [50] E. Bayati, R. Pestourie, S. Colburn, Z. Lin, S. G. Johnson, and A. Majumdar, “Inverse Designed Metalenses with Extended Depth of Focus,” *ACS Photonics*, vol. 7, no. 4, pp. 873–878, Apr. 2020. DOI: 10.1021/acsp Photonics.9b01703.
- [51] S. Hooten, T. V. Vaerenbergh, P. Sun, S. Mathai, Z. Huang, and R. G. Beausoleil, “Adjoint Optimization of Efficient CMOS-Compatible Si-SiN Vertical Grating Couplers for DWDM Applications,” *Journal of Lightwave Technology*, vol. 38, no. 13, pp. 3422–3430, Jul. 2020. DOI: 10.1109/JLT.2020.2969097.
- [52] W. Jin, S. Molesky, Z. Lin, K. M. C. Fu, and A. W. Rodriguez, “Inverse Design of Compact Multimode Cavity Couplers,” *Optics Express*, vol. 26, no. 20, pp. 26 713–26 721, 2018. DOI: 10.1364/oe.26.026713.
- [53] W. Jin, W. Li, M. Orenstein, and S. Fan, “Inverse Design of Lightweight Broadband Reflector for Relativistic Lightsail Propulsion,” *ACS Photonics*, vol. 7, no. 9, pp. 2350–2355, Sep. 2020. DOI: 10.1021/acsp Photonics.0c00768.
- [54] A. Michaels, M. C. Wu, and E. Yablonovitch, “Hierarchical Design and Optimization of Silicon Photonics,” *IEEE Journal of Selected Topics in Quantum Electronics*, vol. 26, no. 2, pp. 1–12, 2020. DOI: 10.1109/JSTQE.2019.2935299.
- [55] P. Sun, T. V. Vaerenbergh, M. Fiorentino, and R. Beausoleil, “Adjoint-method-inspired grating couplers for CWDM O-band applications,” *Optics Express*, vol. 28, no. 3, pp. 3756–3767, Feb. 2020. DOI: 10.1364/OE.382986.
- [56] Z. Lin, C. Roques-Carmes, R. Pestourie, M. Soljačić, A. Majumdar, and S. G. Johnson, “End-to-end nanophotonic inverse design for imaging and polarimetry,” *Nanophotonics*, vol. 10, no. 3, pp. 1177–1187, 2021. DOI: 10.1515/nanoph-2020-0579.
- [57] Z. Omair, S. M. Hooten, and E. Yablonovitch, “Broadband mirrors with >99% reflectivity for ultra-efficient thermophotovoltaic power conversion,” in *Energy Harvesting and Storage: Materials, Devices, and Applications XI*, vol. 11722, International Society for Optics and Photonics, Apr. 2021, p. 1 172 208. DOI: 10.1117/12.2588738.
- [58] D. Vercruyssen, N. V. Sapra, K. Y. Yang, and J. Vučković, “Inverse-Designed Photonic Crystal Devices for Optical Beam Steering,” *arXiv:2102.00681 [physics]*, Feb. 2021.
- [59] Z. Zeng, P. K. Venuthurumilli, and X. Xu, “Inverse Design of Plasmonic Structures with FDTD,” *ACS Photonics*, vol. 8, no. 5, pp. 1489–1496, May 2021. DOI: 10.1021/acsp Photonics.1c00260.
- [60] R. J. Williams, “Simple statistical gradient-following algorithms for connectionist reinforcement learning,” *Machine Learning*, vol. 8, no. 3, pp. 229–256, May 1992. DOI: 10.1007/BF00992696.
- [61] R. S. Sutton, D. McAllester, S. Singh, and Y. Mansour, “Policy Gradient Methods for Reinforcement Learning with Function Approximation,” in *Advances in Neural Information Processing Systems*, S. Solla, T. Leen, and K. Müller, Eds., vol. 12, MIT Press, 2000.
- [62] A. Michaels, *EMopt*, May 2019. [Online]. Available: <https://github.com/anstmichaels/emopt>.
- [63] L. Faury, F. Vasile, C. Calauzènes, and O. Fercoq, “Neural Generative Models for Global Optimization with Gradients,” *arXiv:1805.08594 [cs]*, May 2018.

- 
- [64] L. Faury, C. Calauzenes, O. Fercoq, and S. Krichen, “Improving Evolutionary Strategies with Generative Neural Networks,” *arXiv:1901.11271 [cs]*, Jan. 2019.
  - [65] N. Hansen, “The CMA Evolution Strategy: A Tutorial,” *arXiv:1604.00772 [cs, stat]*, Apr. 2016.
  - [66] T. Salimans, J. Ho, X. Chen, S. Sidor, and I. Sutskever, “Evolution Strategies as a Scalable Alternative to Reinforcement Learning,” *arXiv:1703.03864 [cs, stat]*, Sep. 2017.
  - [67] H. Ghraieb, J. Viquerat, A. Larcher, P. Meliga, and E. Hachem, “Single-step deep reinforcement learning for open-loop control of laminar and turbulent flows,” *Physical Review Fluids*, vol. 6, no. 5, p. 053902, May 2021. DOI: 10.1103/PhysRevFluids.6.053902.
  - [68] T. Watanabe, M. Ayata, U. Koch, Y. Fedoryshyn, and J. Leuthold, “Perpendicular Grating Coupler Based on a Blazed Antireflection Structure,” *Journal of Lightwave Technology*, vol. 35, no. 21, pp. 4663–4669, 2017. DOI: 10.1109/JLT.2017.2755673.